Journal of Biomechanics 48 (2015) 3004–3011

Contents lists available at ScienceDirect

Journal of Biomechanics

journal homepage: www.elsevier.com/locate/jbiomech
www.JBiomech.com

Tribology studies of the natural knee using an animal model in a new whole joint natural knee simulator

Aiqin Liu [a,*], Louise M Jennings [a], Eileen Ingham [b], John Fisher [a]

[a] Institute of Medical and Biological Engineering, School of Mechanical Engineering, Faculty of Engineering, University of Leeds, Leeds, UK
[b] Institute of Medical and Biological Engineering, School of Biomedical Sciences, Faculty of Biological Sciences, University of Leeds, Leeds, UK

ARTICLE INFO

Article history:
Accepted 29 July 2015

Keywords:
Tribology
Friction
Natural knee joint
Cartilage
Simulator

ABSTRACT

The successful development of early-stage cartilage and meniscus repair interventions in the knee requires biomechanical and biotribological understanding of the design of the therapeutic interventions and their tribological function in the natural joint. The aim of this study was to develop and validate a porcine knee model using a whole joint knee simulator for investigation of the tribological function and biomechanical properties of the natural knee, which could then be used to pre-clinically assess the tribological performance of cartilage and meniscal repair interventions prior to *in vivo* studies. The tribological performance of standard artificial bearings in terms of anterior–posterior (A/P) shear force was determined in a newly developed six degrees of freedom tribological joint simulator. The porcine knee model was then developed and the tribological properties in terms of shear force measurements were determined for the first time for three levels of biomechanical constraints including A/P constrained, spring force semi-constrained and A/P unconstrained conditions. The shear force measurements showed higher values under the A/P constrained condition (predominantly sliding motion) compared to the A/P unconstrained condition (predominantly rolling motion). This indicated that the shear force simulation model was able to differentiate between tribological behaviours when the femoral and tibial bearing was constrained to slide or/and roll. Therefore, this porcine knee model showed the potential capability to investigate the effect of knee structural, biomechanical and kinematic changes, as well as different cartilage substitution therapies on the tribological function of natural knee joints.

1. Introduction

Current total knee replacement (TKR) surgery for the treatment of degenerative joint disease is highly successful in patients over 65 with relatively low demands, with success rates over 90% at ten years (Ranawat et al., 1993; Laskin, 2001; Pavone et al., 2001; Rodriguez et al., 2001). Knee replacement is, however, less effective for young patients with expectations of an active life style and the desire to maintain normal function. There is an increasing clinical need for effective therapies for young patients with acute injuries or early degenerative disease in the knee, such as cartilage substitution therapies and meniscal repair interventions. The successful development of such interventions in the knee is dependent on an understanding of the biomechanical and biotribological function of the design of the interventions and their tribological function within the natural joint. In particular, there is a paucity of knowledge of how the range of variables in the natural knee and the design parameters of the intervention interact to determine tribological function. Computational models have been developed to study time dependent biomechanics and contact mechanics (Meng et al., 2014). Whole natural knee joint experimental simulation systems are needed to investigate tribological function and these will play an important role in extending the understanding of the natural knee as a complex tribological system.

Numerous studies have been carried out to investigate the biotribology of articular cartilage as a material, using simple *in vitro* tribological pin on plate simulation systems. These have been used to evaluate various cartilage replacement biomaterials and therapies lubricants (Forster and Fisher, 1996, 1999; Krishnan et al., 2004; Bell et al., 2006; Carter et al., 2007; Katta et al., 2007; Northwood and Fisher, 2007; Northwood et al., 2007). Simple geometry cartilage specimen tests, however do not represent the tribological response of the whole natural knee as a biomechanical system, cartilage/meniscus interactions and the complexities and interactions of the geometries, loads, motions and resulting kinematics, biomechanics and tribological function. Currently, most knee simulators are designed to study wear of total knee replacements (TKR) and few have been designed to test the whole natural knee (Van Houtem et al., 2006; Sutton et al., 2010; Bedi et al., 2010). To date, there are no published reports on *in vitro* tribological studies of the natural knee joint, which have the

* Corresponding author. Tel.: +44 113 343 9436; fax: +44 113 242 4611.
E-mail address: A.Liu@leeds.ac.uk (A. Liu).

http://dx.doi.org/10.1016/j.jbiomech.2015.07.043

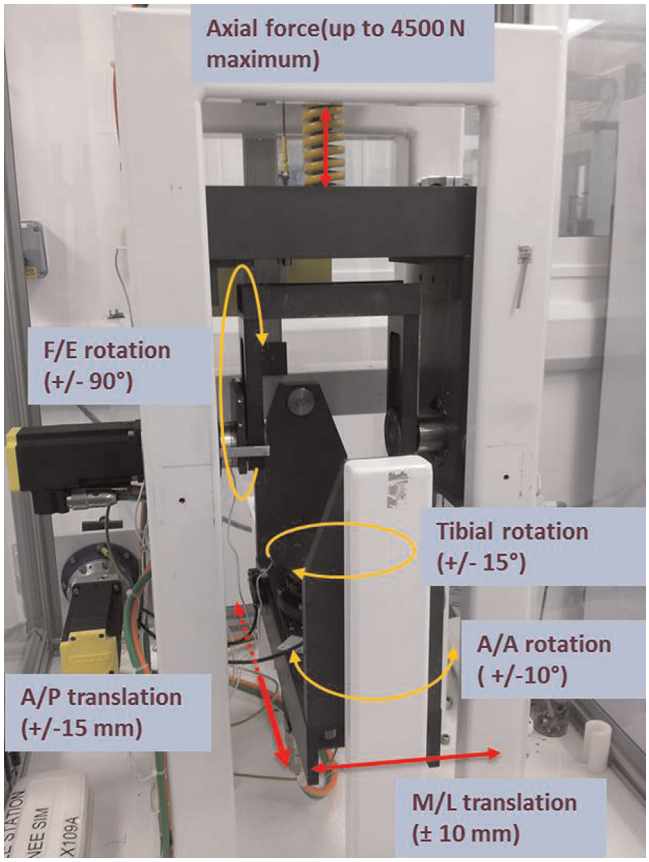

Fig. 1. Overview of the single station natural knee simulator.

capability for *in vitro* pre-clinical testing of early-stage cartilage or meniscal repair interventions. Furthermore, novel surgical interventions for cartilage or meniscal repair will require pre-clinical testing in large animal studies and it will be increasingly important to evaluate these interventions in *in vitro* simulations of tribological and biomechanical function prior to *in vivo* studies in animals.

Therefore, the aim of this study was to develop and evaluate a porcine knee model using a whole joint knee simulator for investigation of the tribological function and biomechanical properties. The model could then be adopted for human knee joints and used to pre-clinically assess the tribological performance of cartilage and meniscal repair interventions prior to *in vivo* studies. A new tribological joint simulator which allows the wear and friction testing of both TKR and whole natural knee joints was developed. The initial commissioning studies were performed by determining tribological properties of standard artificial bearings in terms of anterior–posterior (A/P) shear force in the new simulator *in vitro*. The porcine knee model was then developed and the tribological properties in terms of A/P shear force measurements were determined for the first time for different levels of biomechanical constraints.

2. Materials and methods

2.1. Description of single station whole joint knee simulator

The single station electromechanically operated natural knee joint simulator (Simulation Solutions, Manchester, UK) had six degrees of freedom and five controlled axes of motion as shown in Fig. 1. The axial load was force controlled. Both the flexion/extension (F/E) and abduction/adduction (A/A) were displacement controlled while both anterior/posterior (A/P) displacement and the tibial rotation could be controlled using either force or displacement inputs. Medial/lateral (M/L) displacement was not controlled and could be adjusted and fixed to give a specific displacement. The knee flexion/extension could be varied from $+90^{\circ}$ to -90°, which allowed deep flexion movement. The wear of the natural knee could be determined using the simulator and the shear force behaviour (and indirectly friction) in the sagittal plane at either side of the bearings could be monitored. The shear force could be measured on the A/P axis under the tibial tray (445 N load cell, RDP, UK, accuracy: ± 1.3 N) coupled with a low friction sliding bearing.

2.2. Standard control bearings

In order to validate the simulator, standard artificial bearings, which consisted of a stainless steel 303 L cylinder (radius 25 mm) articulating against a polyethylene flat (GUR 1050) were set up to assess the ability of the knee simulator to deliver the kinematic inputs and to determine the A/P shear force at the articulating interface for different conditions of constraint for A/P motion (translation) (Fig. 2a).

2.3. Porcine knee joints

Six porcine knee joints of similar size taken from the right hind leg were obtained from 9 months old Large White pigs within 24 h of slaughter. The porcine leg was dissected by carefully removing soft tissues and all ligaments leaving only the cartilage and meniscus in place. The centre of rotation was determined using a

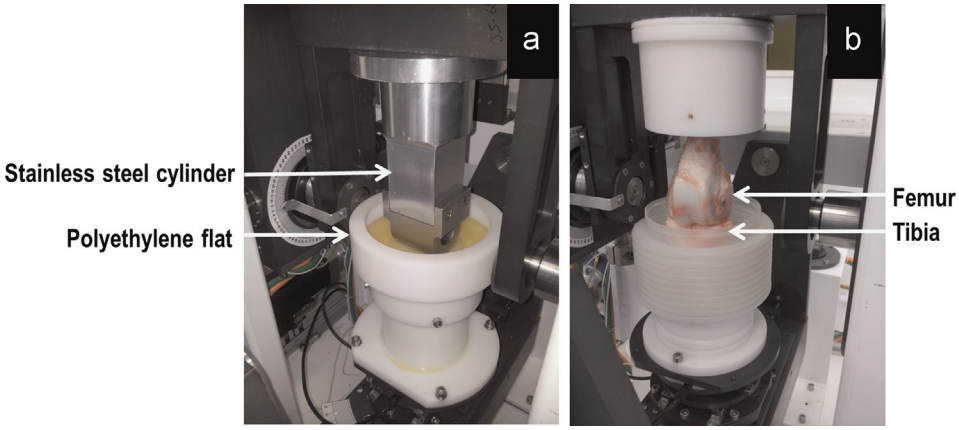

Fig. 2. (a) A standard bearing configuration set up in the single station knee simulator; (b) a porcine knee joint mounted to the single station knee simulator.

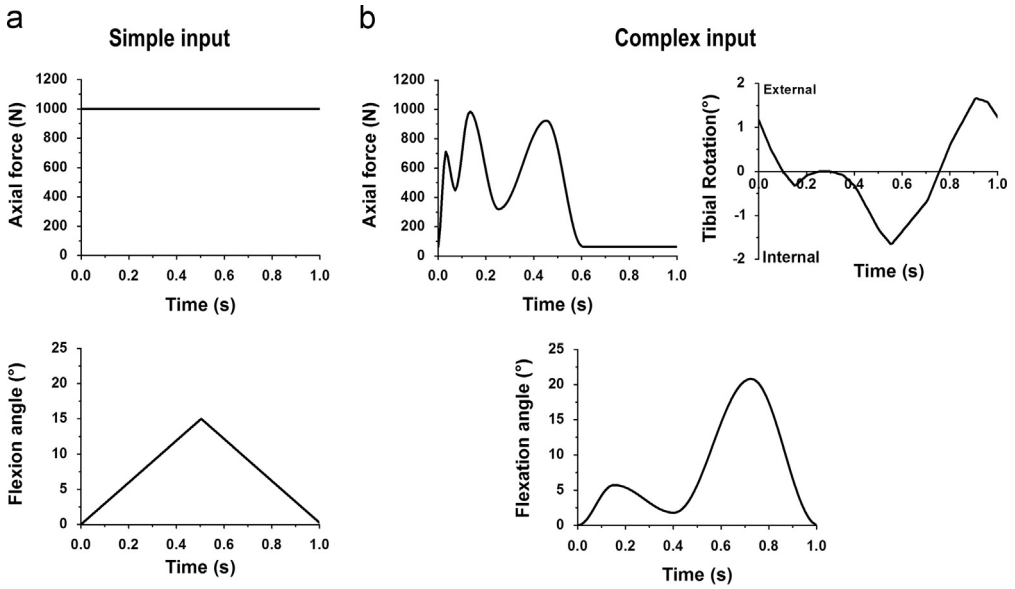

Fig. 3. Kinematic input profiles. (a) Simple input profile: a constant load of 1000 N and flexion/extension from 0° to 15° (b) complex input profile: based on a standard dynamic gait cycle and appropriately scaled for a porcine knee joint.

template methodology according to our previous study (Mccann et al., 2008). Both the femur and tibia were cemented in custom-build pots using polymethylmethacrylate (PMMA; WHW Plastics, UK) (Fig. 2b). Throughout the procedure the soft tissues were kept moist using phosphate buffered saline (PBS; MP Biomedicals, UK). As recommended by ISO 14243-3, the axial force axis was shifted medially by 0.07 of the tibial width (approximately 4.5 mm) by sliding the tibial pot in the fixture with the aim of causing greater medial compartment loading. The cemented porcine knee joint was mounted to the single knee simulator as shown in Fig. 2b.

2.4. Measurement of A/P shear force in A/P direction

Two types of kinematic input profiles were applied in this study (Fig. 3). A simple input profile applied a constant axial force (A/F) of 1000 N and a cyclic triangular flexion/extension (F/E) wave from 0° to 15°. A complex input profile scaled the high kinematic Leeds knee input profiles (Mcewen et al., 2005) to the kinematic limits of porcine knee tissue. The magnitude of the peak load in the load profile was 1000 N and the F/E angles varied from 0° to 21°. Tibial rotation was driven from −1.6° to 1.6° for the complex input profile. The abduction/adduction (A/A) motion was left unconstrained while the medial/lateral (M/L) displacement was constrained in all instances. The anterior/posterior (A/P) motor was not driven in any of the tests, however, three levels of A/P constraint were used to produce different sliding–rolling behaviours in the bearings as follows: (1) Sliding condition, which was created by constraining the tibial A/P carriage; (2) Rolling condition, which was created by decoupling the tibial A/P carriage (unconstrained); (3) A combination of sliding and rolling conditions was created by the incorporation of springs (K=2.69 N mm^{-1}) to constrain the A/P motion. Fig. 4 shows the A/P constrained, spring, and A/P unconstrained test configurations and how the A/P shear force transducer was configured to determine the A/P shear force being transmitted from the femur to the tibia. The tribological behaviour in terms of A/P shear force between the femur and tibia along the A/P axis was determined under these conditions. Each kinematic profile was programmed to apply 300 cycles at a frequency of 1 Hz. The lubricant used was 25% (v/v) new born calf serum (MP Biomedicals, UK). The standard bearing tests were repeated six times using the same components. The simulator outputs including A/F, A/P displacement, F/E displacement, tibial rotational (T/R) displacement and A/P shear force from each test were exported to an Excel spreadsheet for analysis. In order to compare the differences of shear force amongst the three A/P conditions, shear forces at

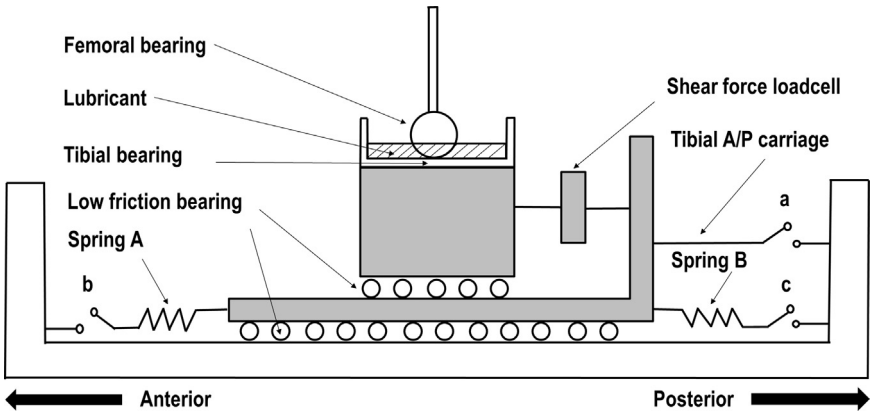

Fig. 4. A schematic illustration showing A/P constrained, spring, and A/P unconstrained test configurations: (1) A/P constrained condition, created when Switch a is on; (2) spring condition, created when Switch b and c are both on while Switch a is off; (3) A/P unconstrained condition, created when Switch a, b, and c are off. The shear force loadcell recorded force generated along the A/P axis under these conditions.

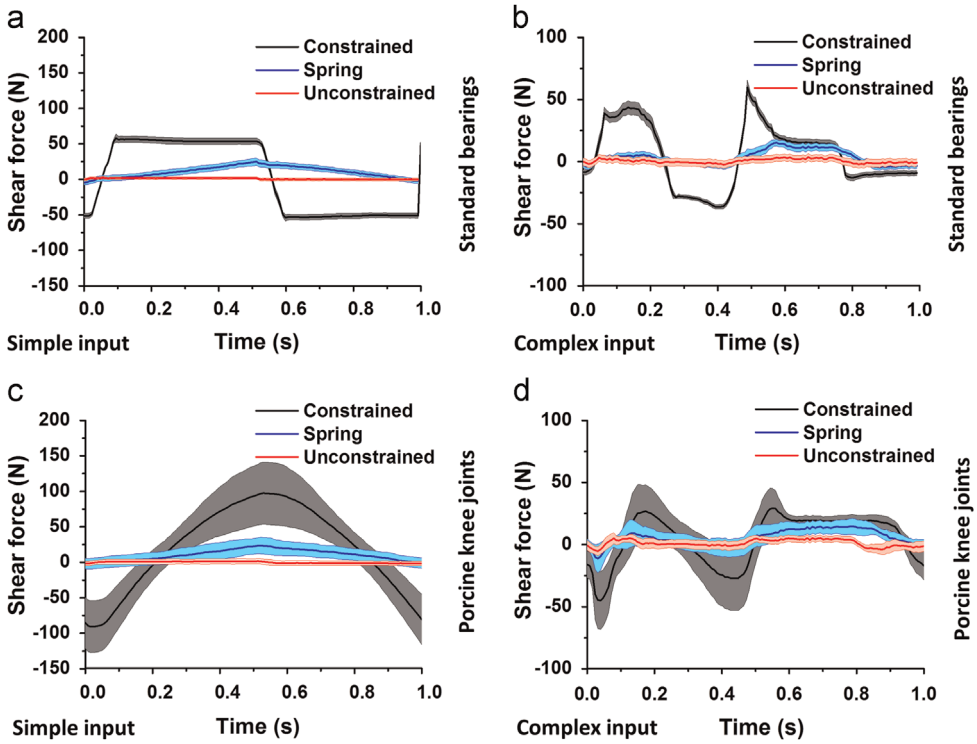

Fig. 5. Average shear forces during standard bearing testing and porcine knee joint testing under (a) and (c) simple input profile with a constant load and flexion/extension only; (b) and (d) complex input profile based on a standard gait cycle and appropriately scaled for a porcine joint. The grey, blue and red regions indicate 95% confidence intervals of the mean ($n=6$) shear force under A/P constrained, spring and A/P unconstrained conditions respectively. (For interpretation of the references to colour in this figure legend, the reader is referred to the web version of this article.)

different time points were recorded and compared. The time points of 0.3 s and 0.7 s under simple input and the time points of 0.1 s, 0.2 s, 0.3 s, 0.6 s, 0.8 s and 0.9 s under complex input were chosen when the shear force at those time points were in relatively steady states. The anterior shear force was taken to be negative.

2.5. Statistical analysis

The average A/P shear force with 95% confidence limits was calculated under the three A/P conditions. The shear forces amongst the three A/P conditions at different time points during the gait cycle were compared using one-way ANOVA, followed by calculation of the minimum significant difference ($p=0.05$) using the *T*-test. Data was plotted as the mean ($n=6$) $\pm$95% confidence limits.

3. Results

3.1. Shear force measurement from standard bearing tests

The six tests showed good repeatability in the three A/P conditions under both 'simple input' and 'complex input' kinematic conditions (Fig. 5a and b). As shown in Fig. 5a, for the simple input condition, the shear force maintained a steady high value (56.7 $\pm$ 4.2 N) under the A/P constrained condition (pure sliding) and a polarity change occurred

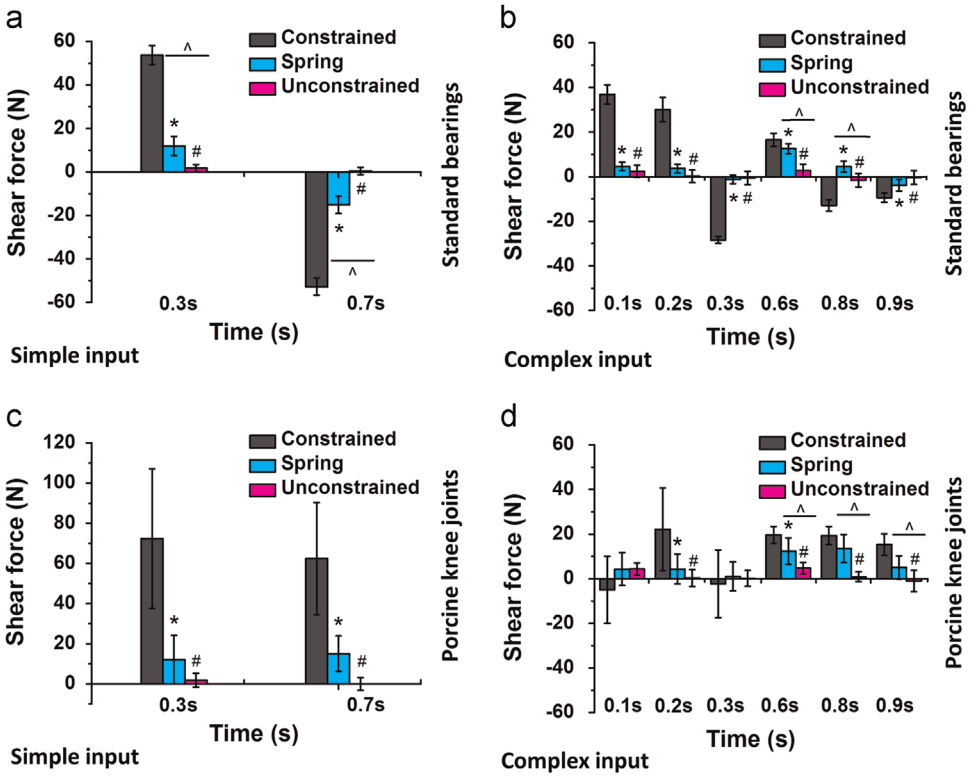

Fig. 6. Comparison of the shear force under different A/P conditions at different time points for standard bearing and porcine knee joint tests under (a) and (c) simple input profile with a constant load and flexion/extension only; (b) and (d) complex profile input based on a standard gait cycle and appropriately scaled for a porcine joint.; ∗ indicates a significant difference in the shear force between the A/P constrained and spring conditions. # indicates a significant difference in shear force between the A/P constrained and A/P unconstrained conditions.^ indicates a significant difference in the shear force between the spring and A/P unconstrained conditions ($p < 0.05$). Data are presented as the mean ($n=6$) $\pm$95% confidence intervals.

when the motion direction (F/E) changed. The shear force increased with increasing flexion angle, resulting in a triangular shear force profile with a peak value of 25 ± 4.8 N at maximum flexion under the spring condition, associated with moving to increased sliding motion. The shear force showed a constant low value (2 ± 1.5 N) under the A/P unconstrained condition (rolling motion).

Under the complex input profile, the A/P constrained condition resulted in a markedly higher shear force response compared to the spring and A/P unconstrained conditions (Fig. 5b). The linear constraint from the springs resulted in a similar shaped shear force profile lower in magnitude than that of the A/P constrained condition. The spring condition generated increased shear force values compared to the A/P unconstrained condition, specifically during the swing phase of the gait cycle (in the region 0.62–0.8 s).

3.2. Shear force measurement from porcine knee tests

As shown in Fig. 5c, under the 'simple input' kinematic conditions, the A/P constrained condition displayed increased shear force with increased flexion angle, resulting in a triangular shear force profile with a peak value of 97.4 ± 43.8 N at maximum flexion. The shear force under the spring condition showed a smaller magnitude triangular wave pattern than the A/P constrained condition with a peak value of 23.4 ± 11.8 N at maximum flexion. A shear force profile with constant low values (1.6 ± 3.0 N) was observed under the A/P unconstrained condition.

During a clinically relevant gait cycle, the A/P constrained condition resulted in a higher shear force response with a range from 45.1 ± 22.8 N (at 0.04 s) anteriorly to 29.2 ± 15.8 N (at 0.55 s) posteriorly, compared to the shear force values ranging from 11.2 ± 11.6 N (at 0.03 s) anteriorly to 14.7 ± 6.4 N (at 0.79 s) posteriorly under the spring condition (Fig. 5d). Similar to the standard bearing, the porcine knee joint under the spring condition showed increased shear force values compared to the A/P unconstrained condition, specifically during the swing phase of the gait cycle (in the region 0.62–0.9 s) when the spring was compressed by approximately 2 mm.

3.3. Comparison of shear force at different time points

As shown in Fig. 6a, the shear force from standard bearing tests was significantly different amongst the three A/P conditions at the 0.3 s and 0.7 s time points under simple kinematics ($p < 0.05$). The shear force under the A/P constrained condition at 0.3 s was 53.7 ± 4.4 N when the flexion angle increased to 9.1°. When the flexion angle changed direction and decreased to 9.1° the polarity of the shear force also reversed, although the value of the shear force was not significantly different (52.8 ± 3.9 N at 0.7 s).

The A/P constrained condition resulted in a significantly higher shear force compared to both the spring condition and A/P unconstrained conditions at all of time points under the complex kinematics (Fig. 6b). The shear force varied significantly amongst the three A/P conditions for the standard bearing tests at 0.6 s and 0.8 s time points ($p < 0.05$). Under the spring condition, there was a significantly higher shear force compared to the A/P unconstrained condition at 0.6 s and 0.8 s time points under the complex kinematics.

The results from porcine knee joint tests showed that the A/P constrained condition generated significantly higher values of shear force compared to both the spring condition and the A/P unconstrained condition at 0.3 s and 0.7 s time points under the simple

kinematic input (Fig. 6c). However, there were no significant differences between the shear force measurements from the spring condition and the A/P unconstrained condition at any time points.

The A/P constrained condition displayed significantly higher values of shear force compared to both the spring condition and the A/P unconstrained condition at the 0.2 s and 0.6 s time points under the complex kinematic input (Fig. 6d). Unlike the artificial materials, the porcine knee joint did not generate a significantly higher shear force under the A/P constrained condition compared to the spring condition at 0.8 s and 0.9 s time points.

4. Discussion

The aim of this study was to develop and evaluate a porcine knee model using a whole joint knee simulator for investigation of the tribological and biomechanical properties of the natural knee. Additionally the study focused on the effects of the biomechanical constraints on the resulting kinematics, proportion of rolling and sliding and resultant tribological function.

Numerous studies have reported that a combination of rolling and sliding mechanisms occur between the femoral and tibial surfaces of natural knees *in vivo* (Iwaki et al., 2000; Chhabra et al., 2001; Hollman et al., 2003; Nagerl et al., 2008, 2009; Fekete et al., 2012). It is currently believed that rolling is dominant at low flexion angles up to 20–30°, while sliding becomes prevalent beyond these flexion angles (Nagerl et al., 2008, 2009). Rolling motion is regarded as low friction behaviour, while sliding, which is believed to generate greater shear stress, is thought to increase wear in artificial knees (Blunn et al., 1991). However, this hypothesis has not been directly tested. The ratio of sliding to rolling ratio is considered to be an important parameter in wear testing of TKR materials (Reinholz et al., 1998, Van Citters et al., 2004). Recently, Fekete et al. (2012) reported a high sliding–rolling ratio at 120° of flexion angle and high sliding increased wear.

The level of constraint and resulting sliding rolling ratio, how it influences friction and wear is important in natural knee simulation, and this requires in depth consideration and understanding when conditions such as meniscal damage and interventions such as meniscus repair, which also influence the level of constraint, are being studied. Of course it is not possible to measure A/P shear force generated by motion and friction if ligaments are retained as some of this force is reacted in the ligaments. In this simulation model external constraints which control motion and kinematics were applied, but nevertheless the known reaction force of the spring constraints, (restricting the rolling motion) is measured in the A/P force.

In order to understand how the level of constraint influenced the motion, from rolling (low constraint with low friction) to sliding (higher constraint with higher friction), the shear force was measured during the articulation of both standard bearing materials and the natural porcine knee in the novel single station simulator. This was achieved by operating the simulator using different conditions of A/P constraint. In these studies, a low shear force indicated a rolling motion occurred and an increase in the shear force suggested that sliding motion occurred. Spring constraints have been used previously in joint simulations for artificial knees (Van Houtem et al., 2006) to simulate soft tissue/ligament function, which constrain anterior posterior movement. Therefore, in this study, in an attempt to constrain A/P translation of the tibia and produce combinations of rolling and sliding motions, spring constraints were applied. A summary of forces contributing to the measured A/P shear force under the different A/P conditions from standard bearing tests and porcine knee tests is shown in Table 1.

The values of shear force measured in tests of the standard bearing materials in the simulator indicated that the three A/P conditions used in this study successfully created different combinations of sliding and rolling motions. Using simple kinematic inputs, different shear force profiles were produced under the different A/P conditions. The shear force under the A/P constrained condition displayed a step profile with steady high values due to the constant friction coefficient from the stainless steel cylinder sliding on the polyethylene flat, which indicated that the measured force was sliding friction force (Table 1).

Under spring condition, the presence of the spring would have limited the A/P motion occurring on the polyethylene flat which created both a rolling and sliding motion during test cycles. The resistive force from the spring led to an increase in the shear force measured with increased flexion angle, resulting in a triangular shear force profile. It is important to note that the reaction force from the spring would have contributed to the shear force measurements under the spring constraint condition (Table 1). However, it is easy to isolate the rolling/sliding friction force from the measured shear force by computing the different knowing spring force.

The shear force measured under the A/P unconstrained condition was rolling friction force (Table 1). For polyethylene, rolling friction was much lower than sliding friction.

For the porcine knee joint simple kinematic input tests in the simulator, the shear force waveforms produced under the A/P unconstrained and spring conditions were similar to the waveforms for the standard materials bearings indicating that similar motions occurred. Interestingly, under the A/P constrained condition, a steep triangular waveform of shear force was observed, this is consistent with increased sliding and in addition forces associated with the interaction of the intersection of the complex geometries of the femur and tibia (Table 1), forces which did not occur in the simple cylinder geometry of the standard polyethylene bearing. It is difficult to determine the sliding friction force under the fully constrained condition in the natural knee. However, it is possible to determine the changes of geometries of the femur and tibia by interpreting the changes of measured shear force.

The shear force performance under the complex dynamic kinematic inputs was more complicated compared to the simple constant load kinematic input. The shear force measured when the standard material bearings were tested under the complex kinematics input increased when a high axial load was applied from 0 to 0.5 s. This was consistent with the theoretical prediction for a sliding friction force. Therefore, the measured shear force was sliding friction force under this condition.

Similar to simple input, the spring would have also contributed to the shear force measurements under the spring condition when the complex input was applied (Table 1). The shear force measured under the spring condition was significantly higher than the shear force under the A/P unconstrained condition when the A/P

Table 1
Summary of forces contributing to measured A/P shear force under three A/P conditions from standard bearing tests and porcine knee tests.

Test condition	Standard bearing tests	Porcine knee tests
A/P constrained	Sliding friction force	Sliding friction force, Interaction force from geometries of the femur and tibia
Spring	Sliding and/or rolling friction force, Spring force	Sliding and/or rolling friction force, Spring force, Interaction force from geometries of the femur and tibia
A/P unconstrained	Rolling friction force	Rolling and/or rolling friction force, Interaction force from geometries of the femur and tibia

displacement remained at 2 mm anteriorly from 0.6 to 0.8 s, suggesting that the spring was generating a constant resistance force which resulted in steady values of shear force as shown in Fig. 5b. During this period, the polyethylene flat tibial component was constrained in the A/P direction, therefore, with an increase in the flexion angle, the stainless steel femoral component started to slide on the polyethylene resulting in a similar high value of shear force (12.5 ± 2.2 N) to that observed under the A/P constrained condition (16.5 ± 2.3 N) at 0.6 s.

The difference in the shear force measured in the porcine knee joint tests under the A/P constrained condition was significantly higher than the shear force measured under the spring and A/P unconstrained conditions ($p < 0.05$) when dynamic high axial load (> 400 N) was applied, showing a similar pattern to the standard bearing. While this was consistent with the theory of a sliding friction force, the force could also be due to other interactions forces between the femur and tibia as the complex geometries move relative to each other (Table 1). The shear force under the spring condition was significantly higher than the shear force under the A/P unconstrained condition at 0.6 s, 0.8 s and 0.9 s when the spring would have generated a steady high resistance force.

Under the A/P unconstrained condition, the porcine knee joints generated a low shear force value of 4.4 ± 2.8 N at 0.1 s when high load of 1000 N was applied during the dynamic gait cycle. Not all this A/P shear force was necessarily due to rolling or sliding friction. The complex geometries and motion of the femur and tibia could result in a small direct component of the load being reacted in the A/P direction, which was measured as a component of the A/P shear force (Table 1). However, these forces were small in magnitudes, which resulted in lower measured shear force under A/P unconstrained condition.

The experimental simulation system developed has highlighted the complexities of the interaction of the biomechanical conditions, constraints and the tribological function in the knee, which influence not only friction but also affect damage and wear. It is important to establish the base line tribological function for the natural joint and the factors that influence it, in order to be able to go on to investigate the effect of degeneration and damage and subsequent interventions in the natural knee in the future studies. The complexity of measuring the A/P shear force and attempts to analyse component of that force due to friction is demonstrated in this study. Indeed this is further complicated when the cruciate ligaments are included. Nevertheless the simulation system allows a base line for A/P shear force to be established for the natural joint under different conditions, such that if a surgical or biomaterial intervention is introduced, the change in A/P shear force may be used to interpret the change in interfacial motion friction, which along with measurements of friction and wear can contribute to an understanding of tribological function.

The study has demonstrated the benefits of using spring constraints to control kinematics and rolling and sliding. The next phase of the work will investigate approaches to matching these constraints more closely to the constraints of the ligaments on each individual joint. Nevertheless, under the spring constraint configuration, the A/P shear force does not just measure the friction shear force, and therefore it is important to determine the shear force of the intact joint, before adding an intervention to study the effect of the intervention on shear force and friction. For interventions relating to meniscus repair, these may alter the constraint and biomechanical function as well as the tribological properties and this needs to be taken into account in future study designs for meniscal interventions. For the intact joint with healthy cartilage surfaces and with no constraints or semi constraints, low A/P shear force was recorded, and this was consistent with low friction force. These conditions and measurements act as a useful baseline and negative control, to which the effect of cartilage or meniscus damage and subsequent repair or biomaterial interventions can be compared in future work.

5. Conclusions

An experimental simulation system for the natural knee has been developed. The A/P shear force measurements under both a simple input profile and a clinically relevant gait cycle input showed higher values under the A/P constrained condition where sliding motion occurred, compared to the A/P unconstrained condition where rolling motion occurred. The results indicated that the *in vitro* simulation model was able to simulate and measure different tribological behaviours when the femoral and tibial bearing was constrained to slide or/and roll. The porcine knee model, set up with appropriate constraints and with a baseline established for the natural knee has shown the potential capability to investigate the effect of knee structural, biomechanical and kinematic changes, and different cartilage substitution therapies on the tribological function of the natural knee.

6. Conflict of interest statement

John Fisher is a consultant to DePuy Synthes Joint Reconstruction, Invibio, Tissue Regenix and Simulation Solutions.

Acknowledgements

This work was supported by the EPSRC (Grant no. EP/G012172/1) Programme grant on Tribology of Cartilage Substitution, the Medical Technologies Innovation and Knowledge Centre supported by EPSRC, BBSRC (Grant no. EPI0191031) and Innovate UK and the ERC (Grant no. 267114) advanced Award REGENKNEE. John Fisher is an NIHR Senior Investigator and is supported through The EPSRC centre for Innovative Manufacturing in Medical Devices. Simulation Solutions manufactured the natural knee joint simulator.

References

Bedi, A., Kelly, N.H., Baad, M., Fox, A.J.S., Brophy, R.H., Warren, R.F., Maher, S.A., 2010. Dynamic contact mechanics of the medial meniscus as a function of radial tear, repair, and partial meniscectomy. J. Bone Joint Surg. Am. 92A, 1398–1408.

Bell, C.J., Ingham, E., Fisher, J., 2006. Influence of hyaluronic acid on the time-dependent friction response of articular cartilage under different conditions. Proc. Inst. Mech. Eng. H 220, 23–31.

Blunn, G.W., Walker, P.S., Joshi, A., Hardinge, K., 1991. The dominance of cyclic sliding in producing wear in total knee replacements. Clin. Orthop. Relat. Res. 273, 253–260.

Carter, M.J., Basalo, I.M., Ateshian, G.A., 2007. The temporal response of the friction coefficient of articular cartilage depends on the contact area. J. Biomech. 40, 3257–3260.

Chhabra, A., Elliott, C.C., Miller, M.D., 2001. Normal anatomy and biomechanics of the knee. Sports Med. Arthrosc. Rev. 9, 166–177.

Fekete, G., De Baets, P., Wahab, M.A., Csizmadia, B., Katona, G., Vanegas-Useche, L.V., Solanilla, J.A., 2012. Sliding–rolling ratio during deep squat with regard to different knee prostheses. Acta Polytech. Hung. 9, 5–24.

Forster, H., Fisher, J., 1996. The influence of loading time and lubricant on the friction of articular cartilage. Proc. Inst. Mech. Eng. H 210, 109–119.

Forster, H., Fisher, J., 1999. The influence of continuous sliding and subsequent surface wear on the friction of articular cartilage. Proc. Inst. Mech. Eng. H 213, 329–345.

Hollman, J.H., Deusinger, R.H., Van Dillen, L.R., Matava, M.J., 2003. Gender differences in surface rolling and gliding kinematics of the knee. Clin. Orthop. Relat. Res. 413, 208–221.

Iwaki, H., Pinskerova, V., Freeman, M. a R., 2000. Tibiofemoral movement 1: the shapes and relative movements of the femur and tibia in the unloaded cadaver knee. J. Bone Joint Surg. Br. 82B, 1189–1195.

Katta, J., Pawaskar, S.S., Jin, Z.M., Ingham, E., Fisher, J., 2007. Effect of load variation on the friction properties of articular cartilage. Proc. Inst. Mech. Eng. Part J: J. Eng. Tribol. 221, 455.

Krishnan, R., Kopacz, M., Ateshian, G.A., 2004. Experimental verification of the role of interstitial fluid pressurization in cartilage lubrication. J. Orthop. Res. 22, 565–570.
Laskin, R.S., 2001. The Genesis total knee prosthesis: a 10-year followup study. Clin. Orthop. Relat. Res. 388, 95–102.
Mccann, L., Udofia, I., Graindorge, S., Ingham, E., Jin, Z., Fisher, J., 2008. Tribological testing of articular cartilage of the medial compartment of the knee using a friction simulator. Tribol. Int. 41, 1126–1133.
Mcewen, H.M.J., Barnett, P.I., Bell, C.J., Farrar, R., Auger, D.D., Stone, M.H., Fisher, J., 2005. The influence of design, materials and kinematics on the in vitro wear of total knee replacements. J. Biomech. 38, 357–365.
Meng, Q.E., Jin, Z.M., Wilcox, R., Fisher, J., 2014. Computational investigation of the time-dependent contact behaviour of the human tibiofemoral joint under body weight. Proc. Inst. Mech. Eng. Part H: J. Eng. Med. 228, 1193–1207.
Nagerl, H., Frosch, K.H., Wachowski, M.M., Dumont, C., Abicht, C., Adam, P., Kubein-Meesenburg, D., 2008. A novel total knee replacement by rolling articulating surfaces. In vivo functional measurements and tests. Acta Bioeng. Biomech. 10, 55–60.
Nagerl, H., Walters, J., Frosch, K.H., Dumont, C., Kubein-Meesenburg, D., Fanghanel, J., Wachowski, M.M., 2009. Knee motion analysis of the non-loaded and loaded knee: a re-look at rolling and sliding. J. Physiol. Pharmacol. 60, 69–72.
Northwood, E., Fisher, J., 2007. A multi-directional in vitro investigation into friction, damage and wear of innovative chondroplasty materials against articular cartilage. Clin. Biomech. 22, 834–842.
Northwood, E., Fisher, J., Kowalski, R., 2007. Investigation of the friction and surface degradation of innovative chondroplasty materials against articular cartilage. Proc. Inst. Mech. Eng. Part H: J. Eng. Med. 221, 263–279.
Pavone, V., Boettner, F., Fickert, S., Sculco, T.P., 2001. Total condylar knee arthroplasty: a long-term followup. Clin. Orthop. Relat. Res. 388, 18–25.
Ranawat, C.S., Flynn Jr., W.F., Saddler, S., Hansraj, K.K., Maynard, M.J., 1993. Long-term results of the total condylar knee arthroplasty. A 15-year survivorship study. Clin. Orthop. Relat. Res. 286, 94–102.
Reinholz, A., Wimmer, M.A., Morlock, M.M., Schnelder, E., 1998. Analysis of the coefficient of friction as function of slide-roll ratio in total knee replacement. J. Biomech. 31, 8.
Rodriguez, J.A., Bhende, H., Ranawat, C.S., 2001. Total condylar knee replacement: a 20-year followup study. Clin. Orthop. Relat. Res. 388, 10–17.
Sutton, L.G., Werner, F.W., Haider, H., Hamblin, T., Clabeaux, J.J., 2010. In vitro response of the natural cadaver knee to the loading profiles specified in a standard for knee implant wear testing. J. Biomech. 43, 2203–2207.
Van Citters, D.W., Kennedy, F.E.H.C.J., Collier, J.P., Nichols, T.D., 2004. A multi-station rolling/sliding tribotester for knee bearing materials. J. Tribol. 126, 380–385.
Van Houtem, M., Clough, R., Khan, A., Harrison, M., Blunn, G.W., 2006. Validation of the soft tissue restraints in a force-controlled knee simulator. Proc. Inst. Mech. Eng. Part H: J. Eng. Med. 220, 449–456.